Role of a novel domain of the U4/U6.U5 tri-snRNP factor Snu66 in pre-mRNA splicing

Balashankar R

A dissertation submitted for the partial fulfilment of BS-MS dual degree in Science

Indian Institute of Science Education and Research (IISER) Mohali
Sector-81, Mohali-140306, Punjab, India

May 2020

Certificate of Examination

This is to certify that the dissertation titled “Role of a novel domain of the U4/U6.U5 tri-snRNP factor Snu66 in pre-mRNA splicing” submitted by Mr. Balashankar R (Reg. No. MS15192) for the partial fulfilment of BS-MS dual degree program of the Institute, has been examined by the thesis committee duly appointed by the Institute. The committee finds the work done by the candidate satisfactory and recommends that the report be accepted.

Prof. Anand K Bachhawat Dr Rajesh Ramachandran Dr Shravan Kumar Mishra
(Supervisor)

Dated: May 4, 2020

Declaration

The work presented in this dissertation has been carried out by me under the guidance of Dr. Shravan Kumar Mishra at the Indian Institute of Science Education and Research Mohali. This work has not been submitted in part or in full for a degree, a diploma, or a fellowship to any other university or institute. Whenever contributions of others are involved, every effort is made to indicate this clearly, with due acknowledgement of collaborative research and discussions. This thesis is a bonafide record of original work done by me and all sources listed within have been detailed in the bibliography.

Balashankar R
(Candidate)

Dated: May 4, 2020

In my capacity as the supervisor of the candidate's project work, I certify that the above statements by the candidate are true to the best of my knowledge.

Dr. Shravan Kumar Mishra

(Supervisor)

Acknowledgement

I would wish to express my immense gratitude to my mentor and supervisor Dr. Shravan Kumar Mishra. I have been fortunate enough to work under his guidance for more than three years. I thank him for his help, valuable suggestions, patient guidance and enthusiastic encouragement.

My sincere thanks to all the UBL members: Prashant, Poonam, Kiran, Rakesh, Sumanjit, Anupa, Karan, Sandra, Praver, Arundhathi, Bhargesh, Bhavya, Nivedha, Sugatha, Amjad, Azeem and Ankita. My special thanks to Poulami with whom I have worked the most and shared our project and challenging (interesting) times. Sincere thanks to Baidnath Mandal (Vidya) for his help and support in the lab.

I am thankful to my thesis committee members Prof. Anand Bachhawat and Dr. Rajesh Ramachandran for their inputs, help and discussion. Sincere thanks to IISER Mohali, all faculties and DST-INSPIRE for supporting my higher education. Finally, I thank all my friends, teachers and family members for their constant help and immense support in all my endeavours.

Balashankar R

List of figures

Contents

Abstract

Eukaryotic gene expression requires the removal of non-coding introns and splicing of the coding exons, which is executed by the dynamic ribonucleoprotein (RNP) complex, spliceosome. Unlike the group II self-splicing introns, the spliceosome has evolved in such a way that it requires many trans-acting factors in addition to the cis-acting RNA elements. These factors help in the assembly, activation of the spliceosome and regulation of splicing. Snu66 is one such general splicing factor which is a part of the tri-snRNP complex. Here, we report the function of a novel domain termed SIND of Snu66 in RNA splicing. Biochemical and splicing reporter assays show that SIND is a functional domain and is also involved in splicing of introns with non-canonical 5'splice site (5'ss). Splicing assays in the intron-rich fission yeast shows that SIND mutant has a general splicing defect. Therefore, our study indicates the involvement and function of a novel domain of a splicing factor in non-canonical 5'ss utilization as well as splicing in general in intron-rich organisms.

Chapter 1

Introduction

1.1 Pre-mRNA Splicing

Eukaryotic genes are split genes where the protein-coding exons are interrupted by non-coding introns (Breathnach & Chambon, 1981). Therefore, introns need to be removed from the precursor messenger RNA (pre-mRNA) and the exons need to be spliced to yield mature mRNA for gene expression. This process which takes place after or along with transcription (co-transcriptional) (Neufeld et al., 2014) and before translation is called pre-mRNA splicing and is carried out by the mega-Dalton Ribonucleoprotein (RNP) complex, the spliceosome (Fig.1.1). The spliceosome comprises of five small nuclear RNA's (snRNA's) and over seventy proteins in yeast (Fica & Nagai, 2017). Spliceosome unlike other RNP complexes like ribosome is exceptionally dynamic and undergoes extensive conformational as well as compositional changes in each splicing reaction (Fica & Nagai, 2017; Shi, 2017b).

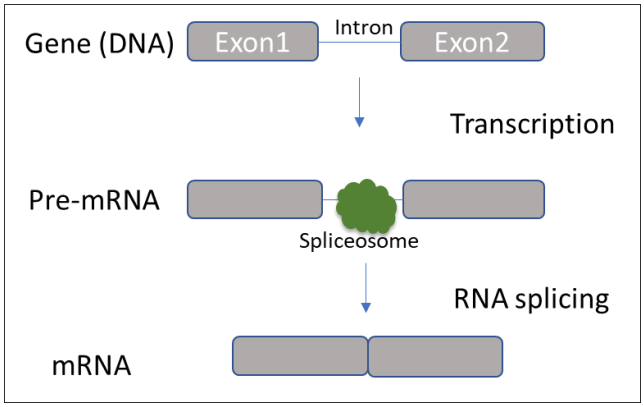

Fig 1.1: RNA splicing: The removal of introns and ligation of exons in a pre-mRNA is executed by the spliceosome to generate functional mRNA's.

1.2 Spliceosome is a protein directed-metalloribozyme

The three conserved sequence elements in a pre-mRNA that are critical for the splicing chemistry are the 5' splice site (5'ss), branch point sequence (BPS) and 3'ss (Wahl et al., 2009). Previous biochemical and metal-rescue experiments have established a two-step phosphoryl transfer mechanism as well as a two-metal ion mechanism for splicing catalysis similar to that

of self-splicing group-II introns (Fica et al., 2013, 2014; Steitz & Steitz, 1993). RNA splicing takes place via two sequential iso-energetic S_N2-type transesterification reactions (Shi, 2017a; Wahl et al., 2009). The first step is the branching reaction where the 2' hydroxyl (2'OH) of the adenine nucleotide of the BPS attacks the phosphodiester group at the 5'ss resulting in a free 5' exon and a lariat intron (where the 5'phosphate of the intron nucleotide 'G' is bound to the 2'Oxygen (2'O) of BP adenosine. In the second step which is the exon ligation, the 3' hydroxyl (3'OH) of the free 5'-exon attacks the 5' end phosphate of the 3'-exon resulting in the ligation of the 5' and 3' exons together and the release of intron lariat. (Fig.1.2)

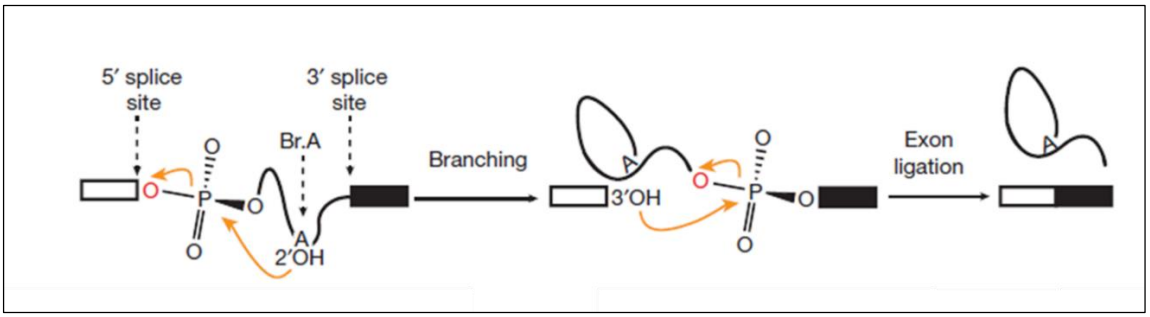

Fig.1.2 (A) Two-step mechanism (branching reaction and exon ligation) of RNA splicing (Figure source: (Fica et al., 2013)).

In the two-step metal ion catalysis, two magnesium ions (Mg^{2+}) known as M1 and M2 in the active site of the spliceosome stabilize the pentacovalent transition states of the two transesterification reactions (Steitz & Steitz, 1993; Wilkinson et al., 2020). In the branching reaction, M1 stabilizes the leaving group (3'OH of last nucleotide of 5' exon) and M2 activates the nucleophile (2'OH of BP adenosine). While in the exon ligation reaction, M1 activates the nucleophile (3'OH of the 5'exon) and M2 stabilizes the leaving group (3'OH of last nucleotide of intron). M1 and M2 that mediates catalysis are bound by phosphates from U6 snRNA establishing that RNA directly mediates catalysis in the spliceosome (Fica et al., 2013, 2014) (Fig. 1.2(B)).

1.3 Spliceosome is a dynamic RNP machine

Recent advances in the field of Cryo-electron microscopy (Cryo-EM) have enormously helped us in understanding the molecular details and mechanisms of splicing at a near atomic resolution. The spliceosome assembles in a stepwise fashion on a pre-mRNA and undergoes

extensive remodelling of the RNA and protein components so as to form the active site for the catalysis.

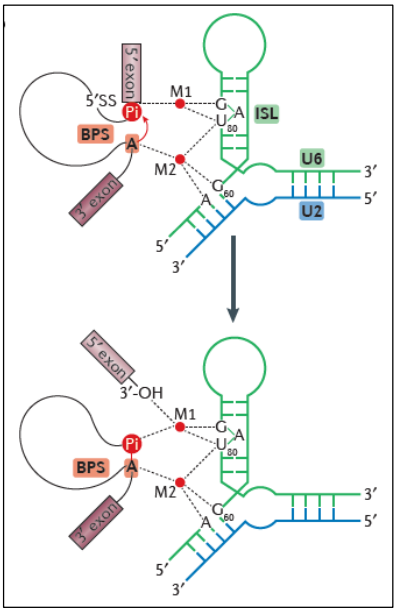

Fig. 1.2 (B): Coordination of M1 and M2 in the two-steps of splicing. U6 snRNA phosphate oxygen atoms coordinate metal ions for the catalysis. (Figure source: (Shi, 2017a).

Decades of biochemical, and genetic experiments have demonstrated the series of assembly and remodelling events that takes place in each splicing cycle. Each splicing reaction can be viewed as a movie where the spliceosome goes through eight functional states for which we now have near atomic resolution cryo-EM snapshots for yeast and human spliceosome (Fig. 1.3). The assembly of the spliceosome starts with the U1 and U2 snRNPS recognizing the 5'ss and the BPS respectively leading to the formation of the E complex and A complex respectively (X. Li et al., 2019; Plaschka et al., 2018). Following A complex formation comes the association of the pre-formed U4/U6.U5 tri-snRNP with the A complex forming the pre-B complex (Plaschka et al., 2017). The U1 snRNP is then released by the DEAD box helicase Prp28 and then the assembly of certain B complex proteins mark the transition of pre-B to B-complex (Bai et al., 2018). The B-complex undergoes extensive conformational rearrangement of RNA-RNA interactions of U2 and tri-snRNP's to get converted to the activated B^{act} complex (Yan et al., 2016). The B^{act} complex then becomes catalytically activated B* complex by Prp2 where the branching reaction takes place (Wan et al., 2019). The B* then becomes step I catalytically activated spliceosome C complex which is converted by Prp16 to step II catalytically activated spliceosome C* which is remodelled for exon ligation (Fatores & Ao, 2011; Fica et al., 2017; Yan et al., 2017). The exon ligation results in post-splicing P complex which further results in the intron-lariat spliceosome (ILS) complex by Prp22 and which is then

disassembled by factors like Prp43 and Brr2 for next round of splicing (S. Liu et al., 2017; Wan et al., 2017) (Fig. 1.3).

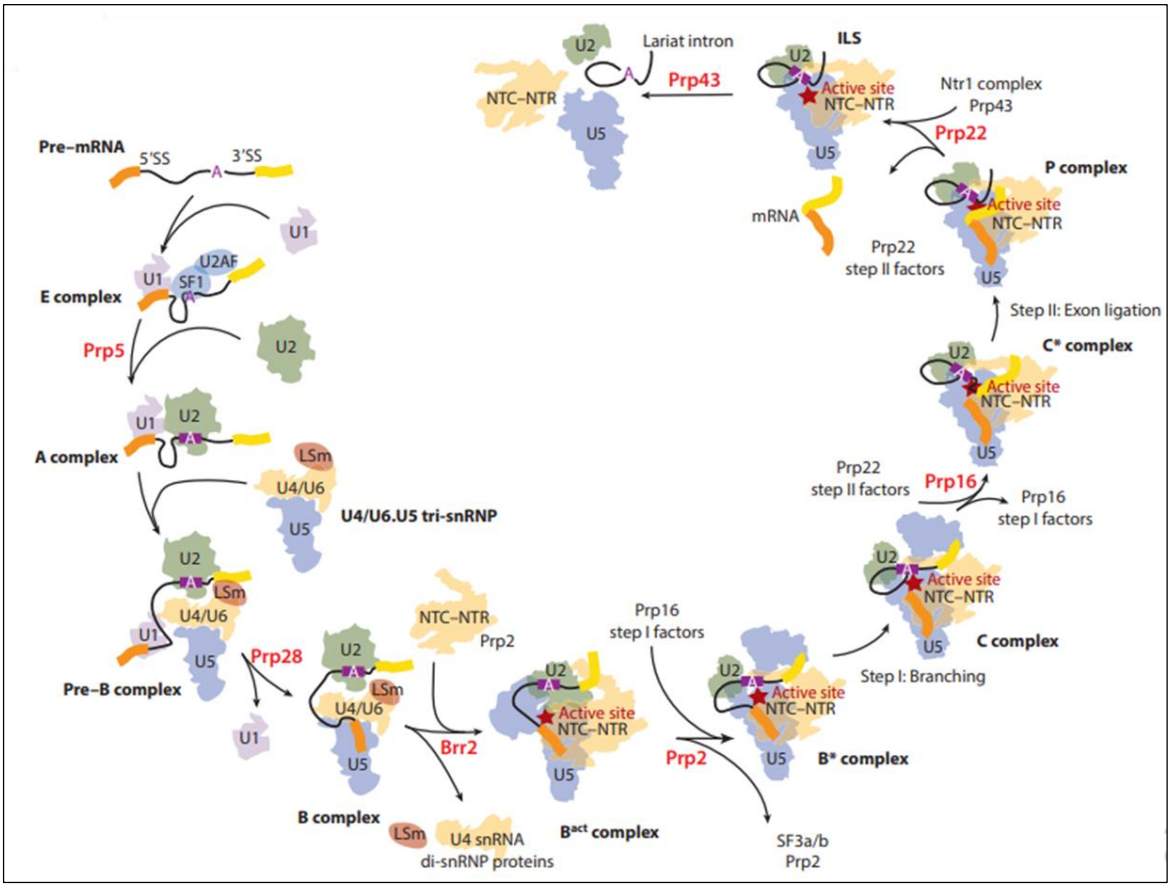

Fig.1.3 Assembly and catalytic cycle of the spliceosome showing the eight functional states of the spliceosome. (Figure source: (Wilkinson et al., 2020).

1.4 The U4/U6.U5 tri-snRNP and Spliceosome activation

As mentioned earlier, the incorporation of the tri-snRNP to the A complex leads to a series of extensive remodelling events within the spliceosome that results in spliceosome activation and formation of the catalytic centre. The release of U1 snRNP by Prp28 converts the pre-B complex to B-complex where in the N-terminus domain of Brr2 then unwinds the U4/U6 duplex following which the conserved ACAGAGA box of U6 pairs with the 5'ss (Plaschka et al., 2017; Staley & Guthrie, 1999). The U2/U6 helix II formed in the B-complex stably holds the tri-snRNP and U2 snRNP on the pre-mRNA and the active site of the spliceosome is formed

during this transition to B^{act} complex together with the incorporation of NTC and NTR proteins (Plaschka et al., 2017).

The correct positioning of 5'ss in the active centre is ensured by the U6 ACAGAGA pairing as well as the U5 loop1 binding to the 5'exon (Fica & Nagai, 2017). The resulting active site of the spliceosome which resembles group II intron active site where the RNA forms catalytic centre has the U6 snRNA forming a catalytic triplex with which the metal ions are coordinated and remains positioned for the two steps of splicing catalysis (Fica et al., 2013, 2014)(Fig. 1.4).

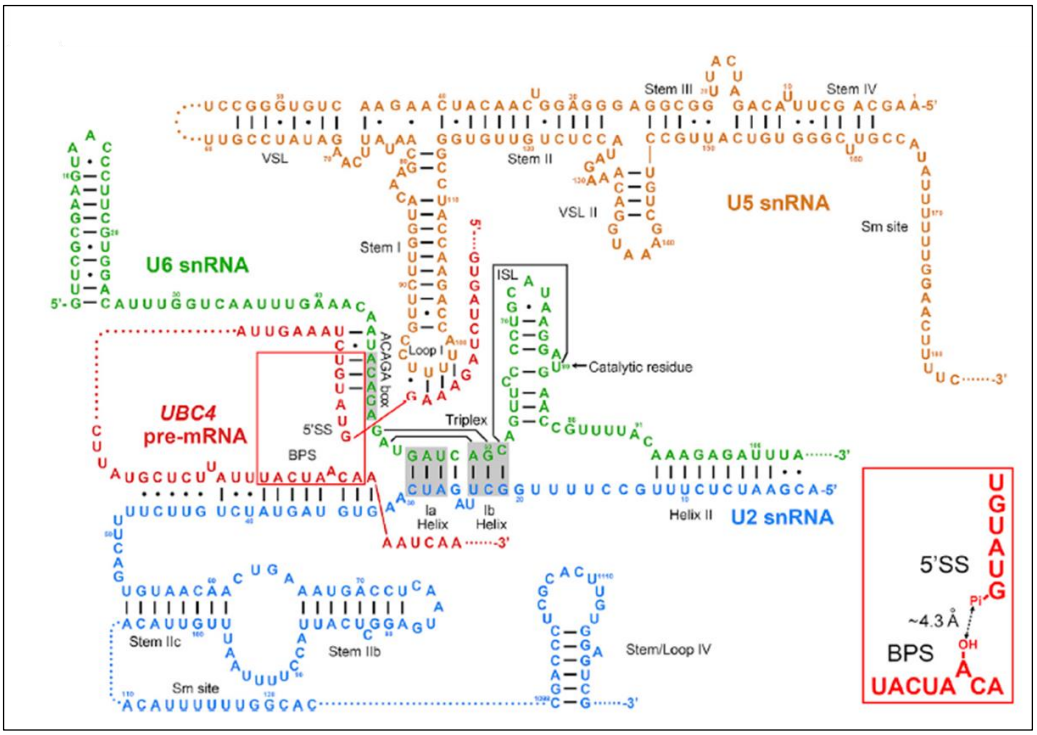

Fig. 1.4 The active site of the spliceosome showing the extensive RNA interaction network formed among the snRNA's and with the pre-mRNA resulting in the active site for catalysis (Figure source: (Wan et al., 2019).

1.5 Snu66

Snu66 is a 66 kDa protein which is a part of the U4/U5.U6 tri-snRNP (Scott W. Stevens & Abelson, 1999). It has been reported to be a non-essential gene at 30°C for budding yeast but becomes essential for viability at lower temperature (16°C) and the cold-sensitive phenotype is because of the defects in pre-mRNA splicing of targets like U3A and U3B snoRNA's (S W Stevens et al., 2001). Snu66 has a homologue in *S. pombe* and Snu66 protein sequence has a significant similarity to human SART1 at its N and C-termini (S W Stevens et al., 2001).

Snu66 has also been reported to be involved in the processing of 5S rRNA precursor and hence functions in 5S rRNA biogenesis (Z. Li et al., 2009).

1.5.1 Snu66 is a tri-snRNP component and a general splicing factor

(Mishra et al., 2011) has reported the presence of HIND (Hub1-INteraction Domain) in Snu66 by which it interacts to the ubiquitin-like protein Hub1 which has a role in non-canonical splice-site usage and alternative splicing. The recent cryo-EM structures of the tri-snRNP at 3.7 A° resolution have revealed that the N-terminus of Snu66 has a globular domain that interacts with Prp8 endonuclease-like and Brr2 N-terminal ratchet domains and that the C-terminus of Snu66 interacts with Brr2-C terminal cassette (Nguyen et al., 2016; Plaschka et al., 2017) (Fig. 1.5). (Charenton et al., 2019) reported that Snu66 holds the association between U4 Sm core domain and the Prp8 RNaseH and Endonuclease domains in the human spliceosome. The human pre-catalytic spliceosome structure also revealed Snu66 having N-terminal domains by which it interacts with Hub1/UBL5 and proteins of spliceosomal core like Prp6, Prp8-linker and RNase H domains and plays a crucial role as a scaffold in the B-complex by stabilizing the two catalytic motifs (switch-loop and beta-finger) of Prp8 (Zhan et al., 2018).

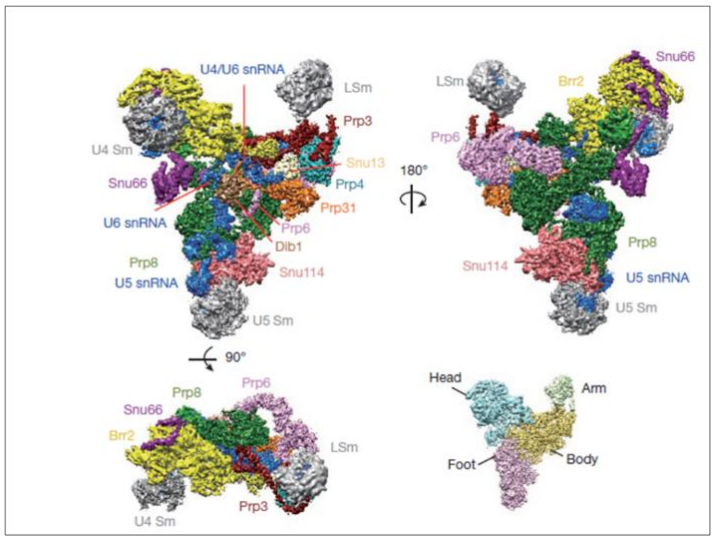

Fig. 1.5. *Saccharomyces cerevisiae* tri-snRNP near atomic model showing Snu66 interaction with spliceosomal core proteins Prp8 and Brr2. (Figure source: (Nguyen et al., 2016).

Although Snu66 has been reported as a general splicing factor and as a part of the tri-snRNP, no study till date has deciphered its precise function in pre-mRNA splicing nor has understood the function of the C-terminus of Snu66. In this study, we try to understand the function of the C-terminus of Snu66 in pre-mRNA splicing. To this end, we have used biochemical approaches and the powerful genetics of two yeast model systems *S. cerevisiae* and *S. pombe*.

1.5.2 Sap1 is a two-hybrid interactor of Snu66

In an yeast two-hybrid (Y2H) screen with Snu66 as a bait, Sap1 was previously identified as an interactor to Snu66 (Shravan Kumar Mishra, unpublished) (Fig. 1.6(A)). Further, we have mapped the interaction of these two proteins from both the sides (Fig. 1.6 (B and C)). Interestingly, when we mapped the interaction from Snu66 side, we found that a 30 amino acid stretch towards the C-terminus of Snu66 is necessary and sufficient for its interaction to Sap1 which we termed SIND for Sap1 INteraction Domain and a protein sequence alignment of SIND across species showed it as a conserved domain from yeasts to humans (Fig. 1.6 (D))

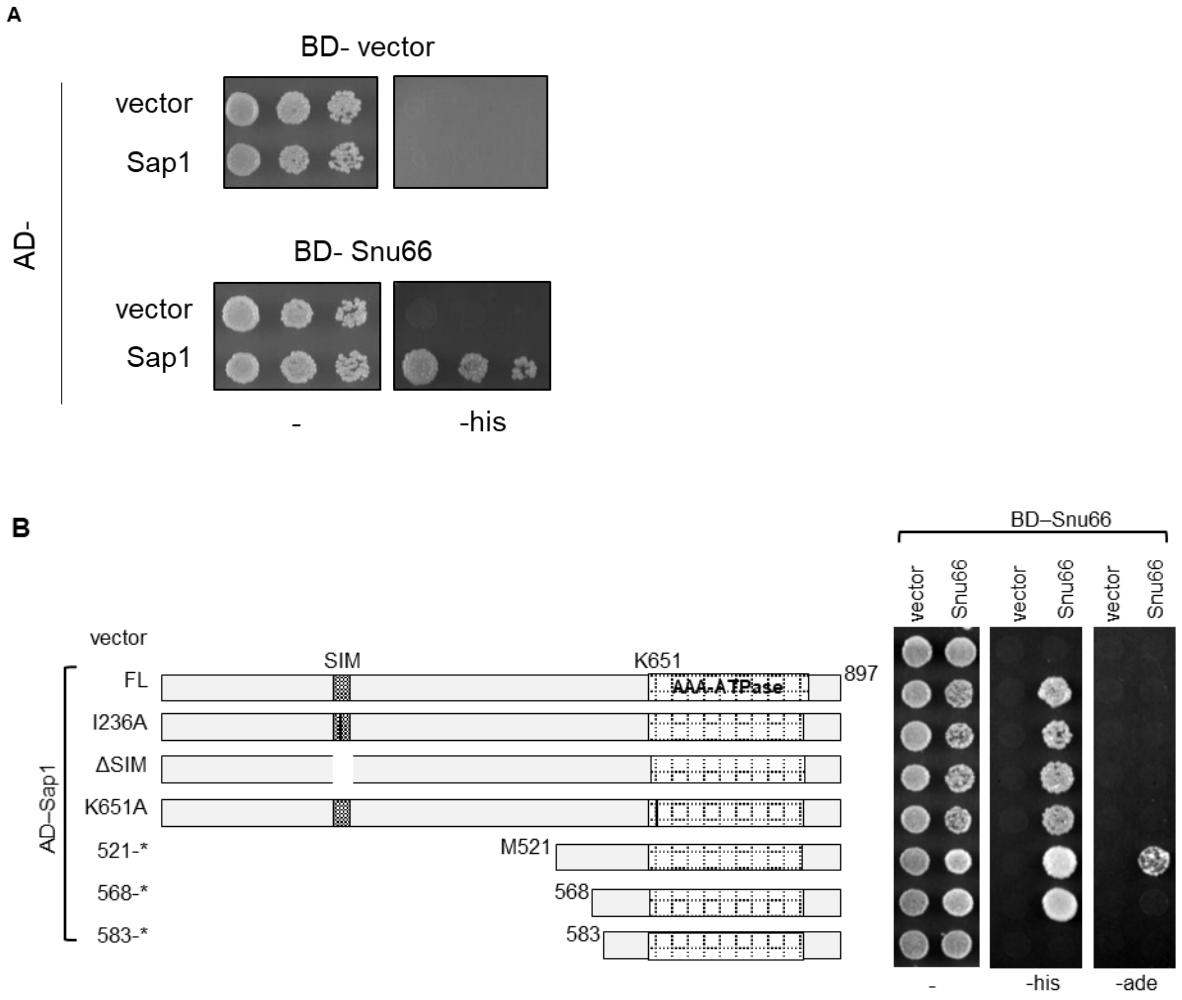

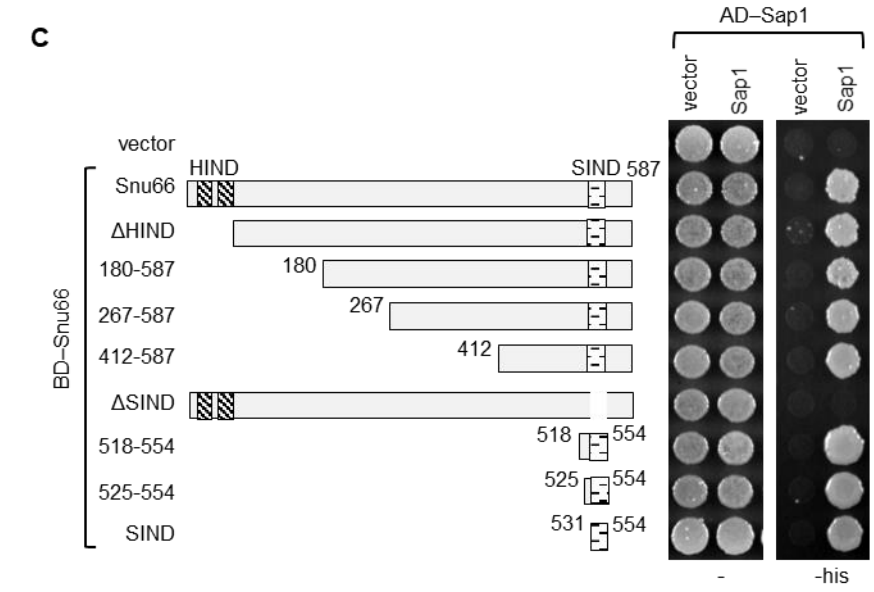

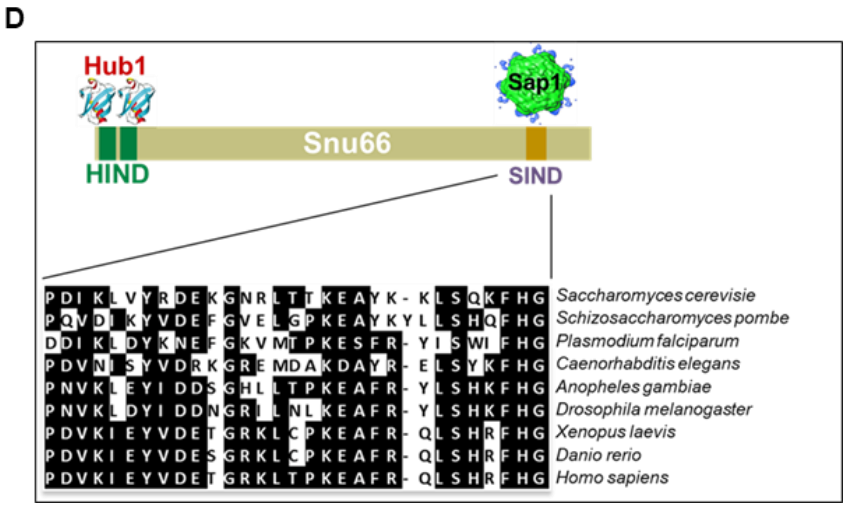

Fig. 1.7 (A) Y2H with BD: Snu66 and AD: Sap1 showing a positive interaction between the two. (B and C) Mapping the interaction of Sap1-Snu66 from a) Sap1 (left panel) side and b) Snu66 side right panel). Y2H assay has been performed for mapping the interaction between the two proteins by generating different point mutants as well as truncations of Sap1 and Snu66. (D) Protein sequence alignment of SIND from different organisms. Snu66-SIND is a conserved domain from yeast to humans.

1.5.3 Objectives of the study:

With these preliminary results, we tried to address the function of this interaction and the function of Sap1- Snu66 complex in RNA splicing. By a series of genetic, biochemical and splicing assays, we were not able to find a function of Sap1 or Sap1-Snu66 interaction in RNA splicing. But interestingly, we realized that the C-term domain of Snu66 which we identified as a conserved domain remained unexplored and there is no report of the function of this domain yet. In this study, we try to address two broad questions:

1. What is the function of the conserved C-terminal SIND of Snu66 in pre-mRNA splicing?
2. What is the mechanism by which Snu66-SIND modifies the spliceosome?

Chapter 2

Experimental Methods

2.1 Plasmid and DNA techniques

The *S. cerevisiae* and *S. pombe* strains and the plasmids used in this study are enlisted in the appendix. The yeast transformation has been done as described in (Knop et al., 1999) . Briefly, 10uL of competent cells were mixed with 1uL of plasmid and 40% PEG (six times the volume) is added. After vortexing, the cells are incubated at 30°C for 30 minutes followed by heat shock of 25 minutes (for *S. cerevisiae*) and 5 minutes (for *S. pombe*) and plated on selection plates and incubated till growth appears.

2.2 Complementation assay

To complement growth defect phenotypes of Δ*snu66* strain in W303 background, competent cells were transformed with respective plasmids and plated on selection plates. The plates were incubated at 30°C till transformants were observed. The transformants were then resuspended in sterile water and OD_{600} was measured. The transformants were diluted at five-fold serial dilution in a microtiter plate and dilution spotting was done on SC- Trp plates. Following spotting, the plates were kept at 16°C, 30°C and 37°C until growth was observed.

2.3 *ACT1-CUP1* reporter assay

The growth of different chromosomal variants of Snu66 in yJU75 genetic background transformed with *ACT1-CUP1* plasmid reporters (harbouring different 5'ss mutations) were monitored in $CuSO_4$ containing media as described in (Lesser & Guthrie, 1993).

2.4 Splicing reporter assay

The splicing reporter assays in *S. pombe* were performed as described in Anil *et al* (unpublished). Site-directed mutagenesis was used to generate variants of the *tho5*-intron in the splicing reporter.

2.5 TCA precipitation and Western blot (WB)

For WB assays, 1 OD_{600} cells of exponentially growing yeasts were harvested and frozen in liquid N_2. Total proteins was isolated by TCA precipitation (Knop et al., 1999). 10ul of the isolated proteins were run on a SDS-PAGE and then transferred to a PVDF membrane followed by blocking and incubation with primary and secondary antibodies at room temperature for 2 and 1 hour respectively. Blots were washed with the 1x TBST buffer and visualised using chemiluminescence detection agent.

2.6 RNA isolation and RT-PCR

RNA isolation followed by cDNA synthesis were done as described in (Inada & Pleiss, 2010) where logarithmically grown yeast cells are harvested at OD_{600}-0.5 at 30°C and also after a heat shock for 15 minutes at 37°C. Total RNA was isolated by the acid phenol method using 15 ml phase-lock gel heavy tubes. Harvested cells were resuspended in acid phenol: chloroform and AES buffer by vortexing. Then the pellets were transferred to 65°C water bath for 7-10 min and vortexed vigorously once every minute. After lysis, cells were incubated on ice for 5 min, and entire organic and aqueous phase was transferred to pre-spun 15 ml phase-lock gel tubes. The tubes were centrifuged at 3000 x g at 4°C for 5 min. Then, PCI was added to the gel tubes, followed by centrifugation. Subsequently, chloroform was added to the supernatant, and after centrifugation, the aqueous phase was transferred into a new 15 ml conical tube with isopropanol and 3 M NaAc. The conical tubes were vortexed thoroughly and 2 ml isopropanol slurry was centrifuged at maximum speed for 20 min at 4°C. After centrifugation, the supernatant was discarded, and RNA pellets were washed two times with 70% ethanol. The RNA pellets were dried in a vacuum concentrator and finally resuspended in nuclease-free water. It was followed by DNase I treatment for 15- 20 minutes at room temperature and Zymo-Spin II column was used for clean-up of RNA. Concentration was measured followed by cDNA synthesis from 2ug isolated RNA was done using RT and random hexamer primer followed by taq PCR using specific primers.

Chapter 3

Results

3.1 Snu66-SIND is a functional domain

Since it has already been reported that the deletion of Snu66 causes cold sensitivity in budding yeast, and there was no report of a domain of Snu66 that is responsible for this phenotype, we tried to identify a functional domain of Snu66 apart from the ones that has already been identified. To this end, we tried to complement the Δ*snu66* cold sensitivity phenotype (in W303 background) by transforming the cells with plasmids harbouring different truncated versions of the *SNU66* gene. It was interesting to see that among the different truncated versions of the gene, the Sap1 binding defective mutant which is the ΔSIND only partially complemented the phenotype indicating that the Δ*snu66* cold sensitivity phenotype partly comes from this domain (Fig.3.1. (A)). Moreover, the double mutant of Hub1 binding defective mutant (ΔHIND) and ΔSIND phenocopied the ΔSIND partial cold sensitivity phenotype (Fig.3.1. (A)). Further to see, whether we can find a point mutant within the SIND stretch that shows a similar phenotype, we analysed the sequence alignment of SIND from *S. cerevisiae and S. pombe* and took two conserved residues at the 533rd and 546th position and mutated them to alanine (D533A and K456A) (Fig.3.1. (B)). We made chromosomal variants of the mutants together with Δ*snu66* and ΔSIND in the yJU17 background and tried to see whether there is any phenotype. There was no partial cold-sensitivity associated with the point mutants unlike ΔSIND. The hub1 binding defective mutant (RRAA) was also included in the assay as a control. This would suggest that the SIND surface of Snu66 is crucial for its splicing function.

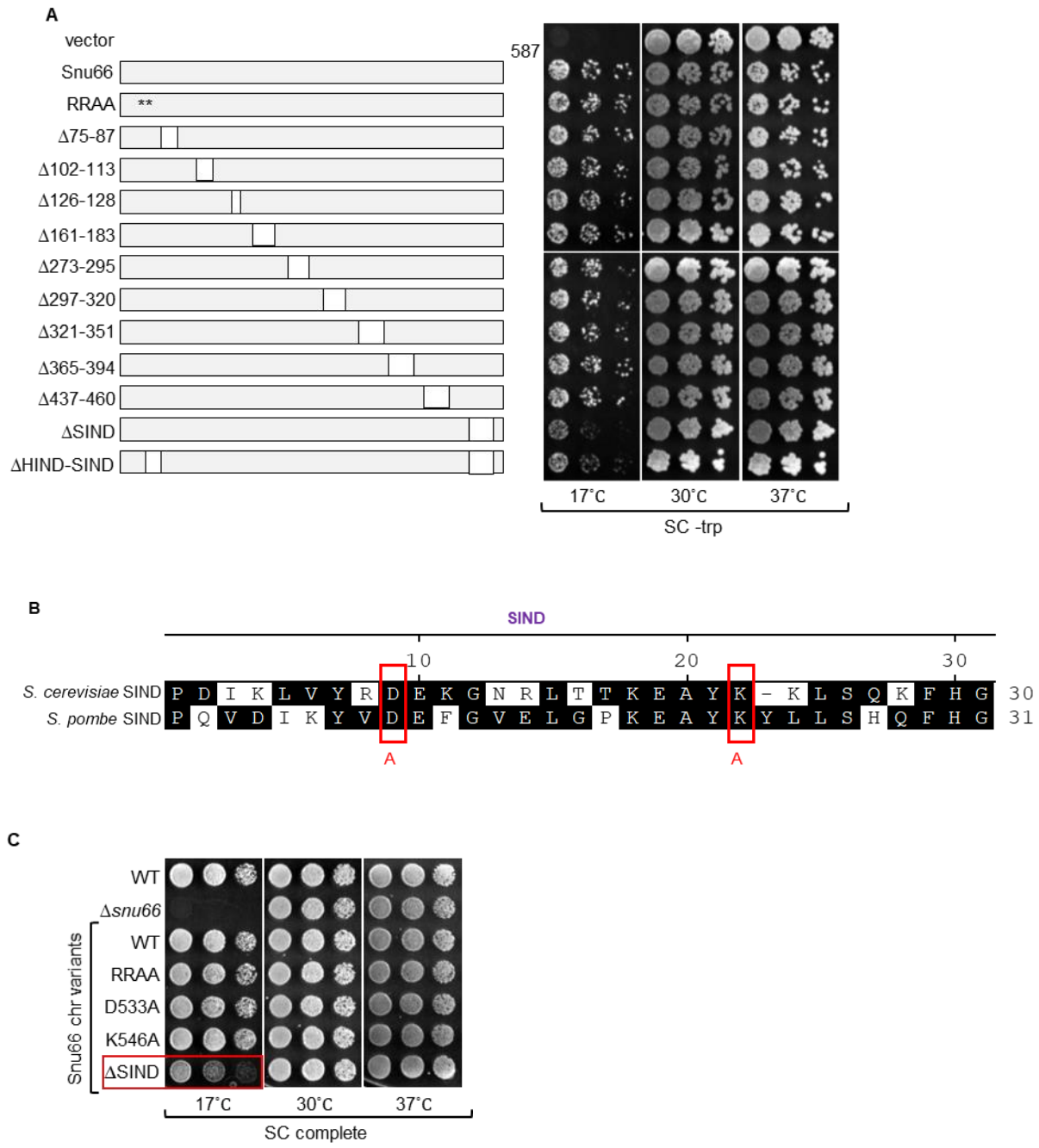

Fig.3.1. (A) Complementation of Δ*snu66* (in W303 yeast genetic background) cold sensitivity phenotype by different truncation versions of *SNU66* gene. Indicated numerical correspond to the amino acid's deletion from *SNU66* ORF. The blank blocks within Snu66 ORF in the schematic correspond to amino acid's deletion (B) The amino acid sequence alignment of SIND of *S. cerevisiae* and *S. pombe*. The indicated red squares show two conserved amino acids for which point mutants to alanine were made. (C) Complementation of the Δ*snu66* phenotype by HIND (RRAA), SIND point mutants and ΔSIND chromosomal variants in yJU17 background.

3.2 SIND plays a role in splicing of introns with non-canonical 5'splice site (5'ss)

In order to address the question of how SIND is involved in splicing, we used a growth based sensitive *ACT1-CUP1* reporter assay. (Mishra et al., 2011) has reported that Δ*snu66* is defective in the usage of non-canonical 5'ss like GUCUGU and GUAUAU although the splicing of the canonical 5'ss GUAUGU is unaffected in Δ*snu66*. We tried to see whether the SIND mutants show a similar defect in the usage of non-canonical 5'splice sites. We have used the different chromosomal variants of Snu66 in yJU17 genetic background for the *ACT1-CUP1* reporter assay. The reporter plasmids harbouring 5'ss variations were transformed with the competent cells of different mutant strains and the transformants were spotted on $CuSO_4$ containing media and the plates were incubated at 30°C for 4 days. The observation that SIND mutants are defective in the usage of a non-canonical 5'ss (discussed in the section 3.2.1) which has a weaker base-pairing interaction with the U6 snRNA attracted us to hypothesise that SIND might help stabilize the U6 snRNA– pre-mRNA interaction in the process of activation of the spliceosome (discussed in section 3.2.2).

3.2.1 SIND mutants are defective in usage of a non-canonical 5'ss

In the *ACT1-CUP1* reporter assay, the SIND mutants are defective in the usage of the 5'ss: GUAUAU and not for the 5'ss: GUCUGU unlike Δ*snu66*. The RRAA mutant also showed a defect specific to the 5'ss: GUAUAU (Fig.3.2.1 (B), (C) and (D).

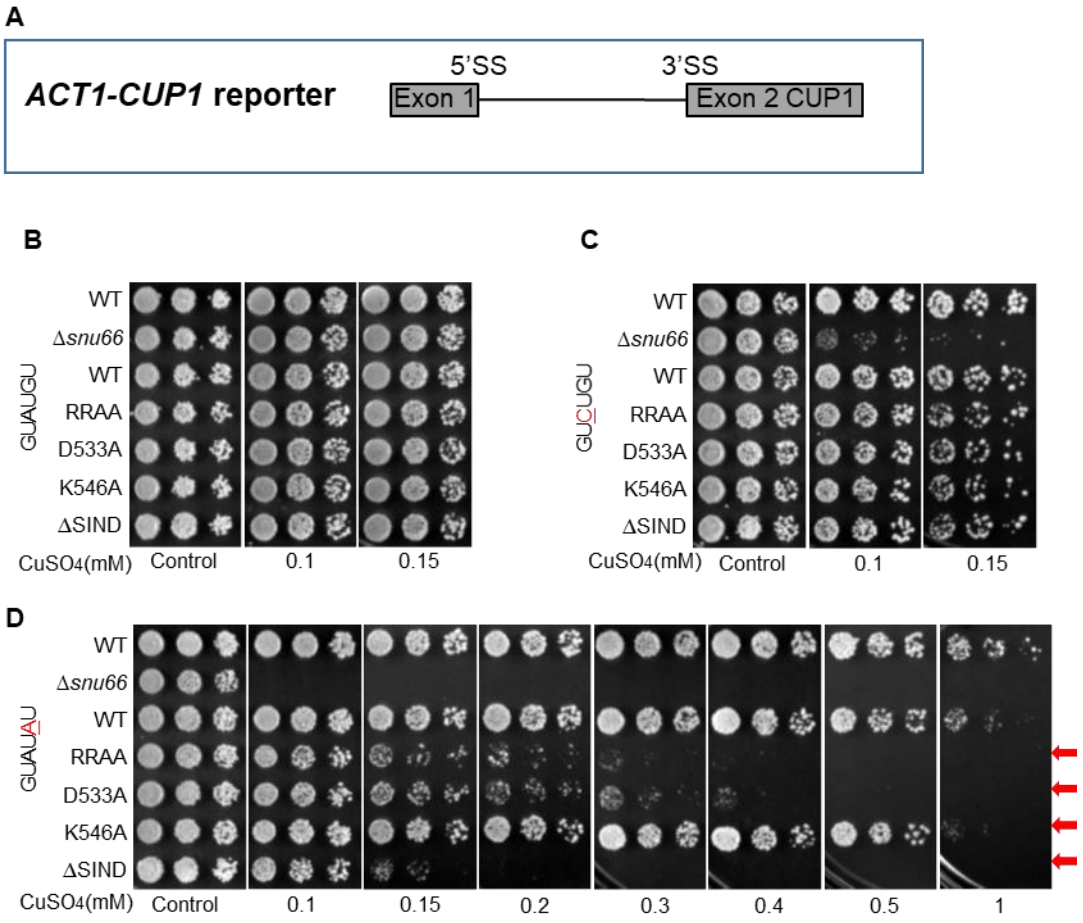

Fig.3.2.1 (A) Schematic of the *ACT1-CUP1* reporter used for the splicing assay (B), (C) and (D) The *ACT1-CUP1* reporter assay for Snu66 chromosomal variants (yJU17 genetic background) with the WT (GUAUGU), GUCUGU and GUAUAU 5'ss respectively (splicing assay with yeast strains transformed with *ACT1-CUP1* constructs harbouring different 5'ss mutations). Equal OD_{600} of cells was spotted on plates containing indicated concentrations of $CuSO_4$ to monitor *CUP1* activity. Plates were incubated at 30°C for 4-5 days. The $CuSO_4$ concentrations were taken till 1 mM for WT and till 0.25 mM for GUCUGU splice site (GUCUGU, being a weak splice site will not get spliced efficiently even in WT with higher [Cu] (data not shown).

3.2.2 Defects in 5'ss usage is not rescued by U6 snRNA mutants

The next question we tried to address was why are SIND mutants defective in the usage of a specific non-canonical 5'ss. We therefore looked at the base-pairing interactions that happen between the non-canonical 5'splice sites and the U1snRNA in the E-complex step as well as with the U6 snRNA after the remodelling by Brr2 in the B to B^{act} transition, it can be seen that GUAUAU has a weak pairing with the U6 snRNA unlike GUCUGU where the pairing is strengthened (Fig.3.2.2 A). Whereas the strength of pairing of the 5'splice sites with the U1

snRNA remained same (Fig.3.2.2 A). Also, since Snu66 is a part of the B-complex, it was more obvious to think that it might work along with U6 snRNA and associated factors so as to help spliceosome attain a structural conformation conducible to accommodate the non-canonical 5'ss into the active centre before the branching reaction. So, we hypothesised that SIND might be a surface that helps in the stabilization of the U6-pairing with the 5'ss prior to catalytic activation of the spliceosome. To test this, we generated plasmid borne variants of the U6 snRNA (WT and mutants that would now pair better with the weak 5'ss GUAUAU). But there was no visible rescue of the GUAUAU splicing defects in RRAA as well as D533A with the U6 mutants that would pair strongly with this 5'ss. However, the possibility of dosage effect (mutants being expressed from a centromeric plasmid and hence very low copy number) and the presence of endogenous U6 snRNA in the experiment can be taken into account and one might still cannot rule out this possibility that SIND works along with U6 snRNP for stabilizing the RNA-RNA interaction.

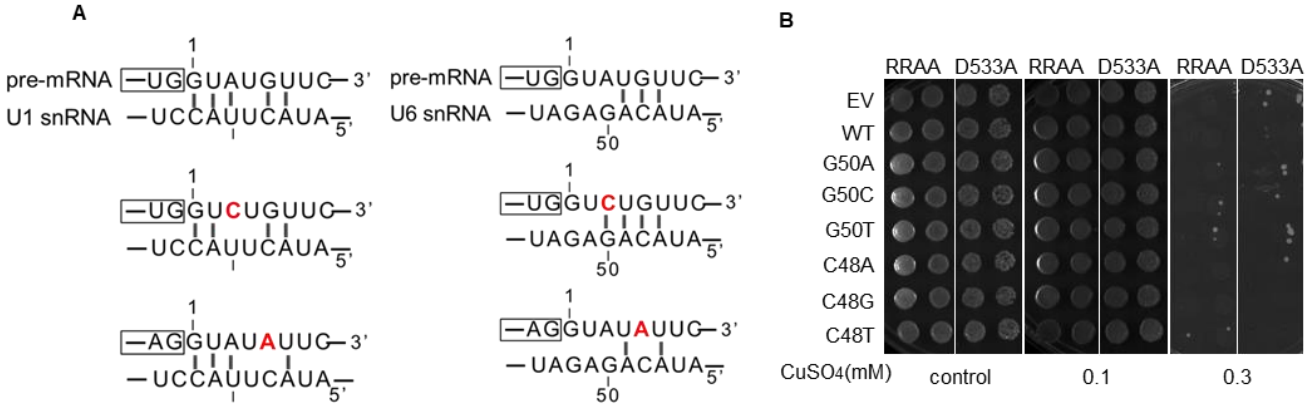

Fig. 3.2.2 (A) Scheme of base-pairing interaction between the 5'ss and U1 snRNA (left panel) and U6 snRNA (right panel of A). (B) The splicing defects in *ACT1-CUP1* reporter assay with the 5'ss: GUAUAU in the RRAA and D533A strains. The strains were co-transformed with the reporter plasmids and the U6 snRNA plasmids. The splicing defects are not rescued by U6 snRNA mutants where the base-pairing strength is increased (mutant G50T and C48T). The other mutants were included in the assay as a control for the experiment and to take into account the possibility of wobble-base pairing that can happen between the base pairs.

3.3 SIND mutant shows general splicing defects in *S. pombe*

To understand the function of SIND in splicing, we took the advantage of a more robust system of intron-rich *S. pombe*. Δ*snu66* in *S. pombe* is lethal, therefore we generated a temperature

sensitive chromosomal mutant of Snu66-SIND termed *snu66-1* which is a lysine to alanine mutation at 613rd position (K613A). We used this strain for the splicing reporter assays as well as the RT-PCR assays.

3.3.1 Monitoring splicing defects using Splicing reporter assays

In order to corroborate the observation that Snu66-SIND mutants are defective in the usage of a non-canonical 5'ss and to gain insights into the function of SIND in an intron-rich organism, we tried to monitor splicing in *S. pombe* using a splicing reporter (Anil et al, unpublished) (Fig.3.4.1 (A). The splicing reporter is constructed in such a way that the *S. pombe ura4* gene is split by inserting an intron of *tho5* gene. Only after the accurate splicing, the Ura4 functional protein will be formed. The growth of cells on uracil lacking media and no growth on the counter selection plate (having 5' FOA) would enable us check whether splicing happens or not. In the growth-based assay for the splicing reporters, there was no obvious splicing defects seen probably because the *ura4* being a very stable protein product though synthesised in minimal amount is sufficient for cell growth (Fig.3.4.1 (B). But the corresponding WB analysis for the reporters show a difference in splicing of *ura4* in *snu66-1* compared to the WT strain in terms of less amount of the full length functional Ura4 protein being formed (Fig.3.4.1(C).

A

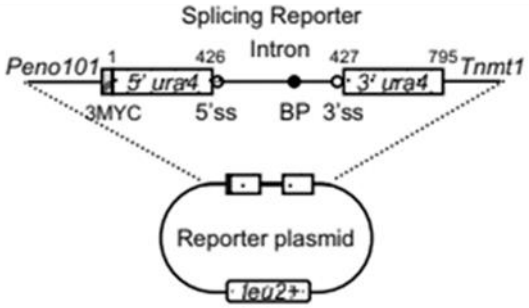

Splicing	Growth on −URA	Growth on +FOA
YES	YES	NO
NO	NO	YES

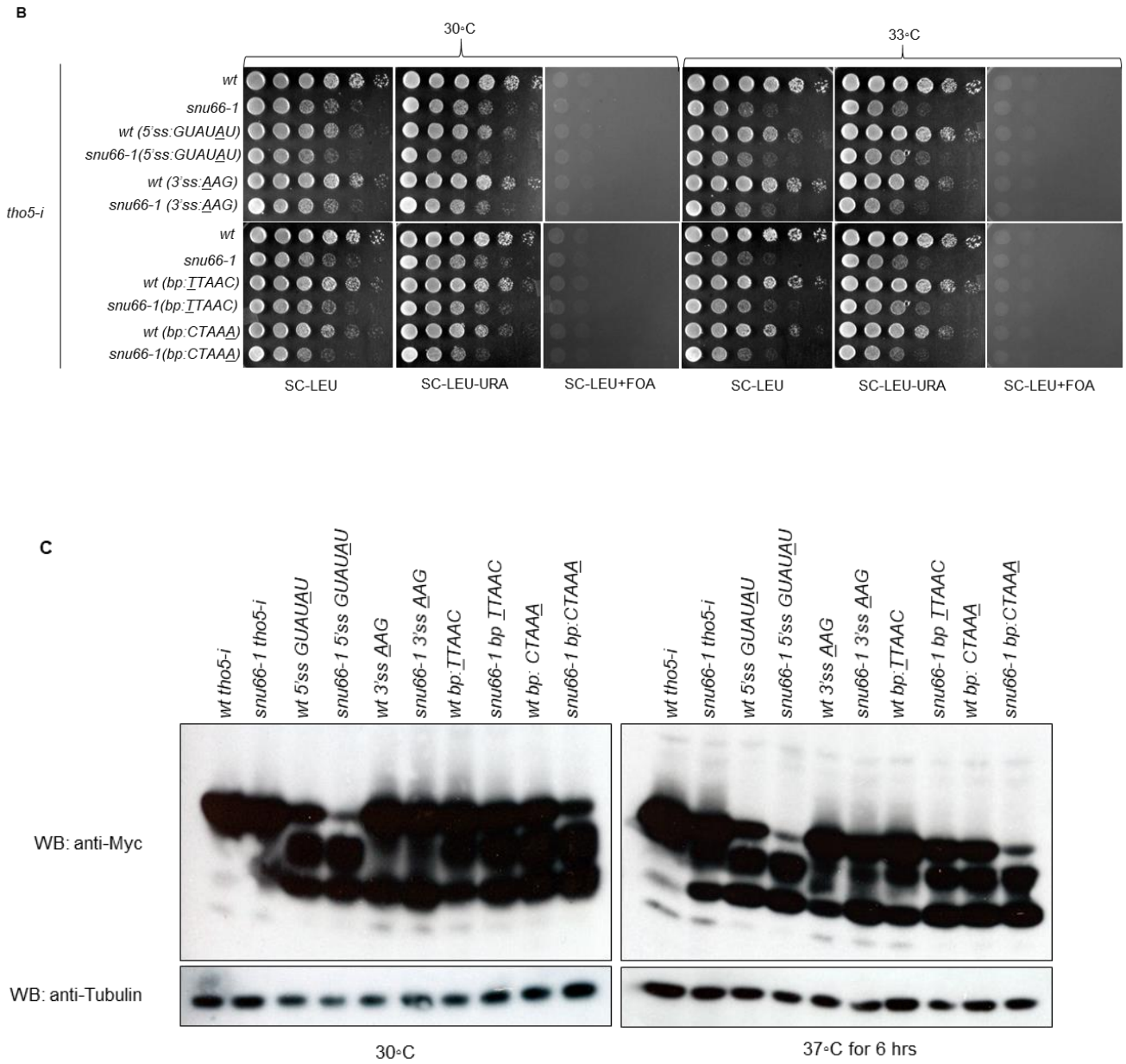

Fig.3.3.1. (A) Schematic showing design of splicing reporters and growth assays (ss, splice site; BP, branch point). (Figure directly adapted from Anil et al (unpublished). (B). Growth based assay for the splicing reporter assay with the wild type and *snu66-1 S. pombe* strain transformed with the splicing reporter plasmids harbouring mutations at 5'ss, BP and 3'ss. No visible growth was observed on the counter-selection FOA plate. (C) The WB assay for the splicing reporters to monitor the splicing defects in the *ura4* gene. There are splicing defects for the different mutants of 5'ss, BP and 3'ss in *snu66-1* strain. The lower band (3rd from top in fig. 3.4.1 (C)) correspond to lower molecular weight peptides arising due to the translation of an *ura4* pre-mRNA that has a pre-mature stop codon in its intron and the middle band might be because of the usage of an alternative 3'ss that exists within the 3'exon of *ura4* .

3.3.2 Monitoring splicing defects using RT-PCR assay

In order to see whether SIND has any specific targets and to see whether any intronic feature can define SIND dependency for splicing, we monitored splicing defects of some *S. pombe* genes with varying intronic features and functions in *snu66-1* strain. Surprisingly, compared to the WT, *snu66-1* shows massive splicing defects for most of the targets we have checked for. The WT and *snu66-1* strain were grown at 30°C and shifted to 37 for 15 minutes. Total RNA was isolated followed by cDNA synthesis and RT-PCR with specific primers for different target genes. The closer analysis of the intron-retention bands for different targets give us a hint to hypothesise that SIND might be required more for splicing where there is weak 5'ss: GUAUAU, weak BPS: CTTAC and where the intron length is comparatively large (>75nt) (further experiments need to be done to establish this).

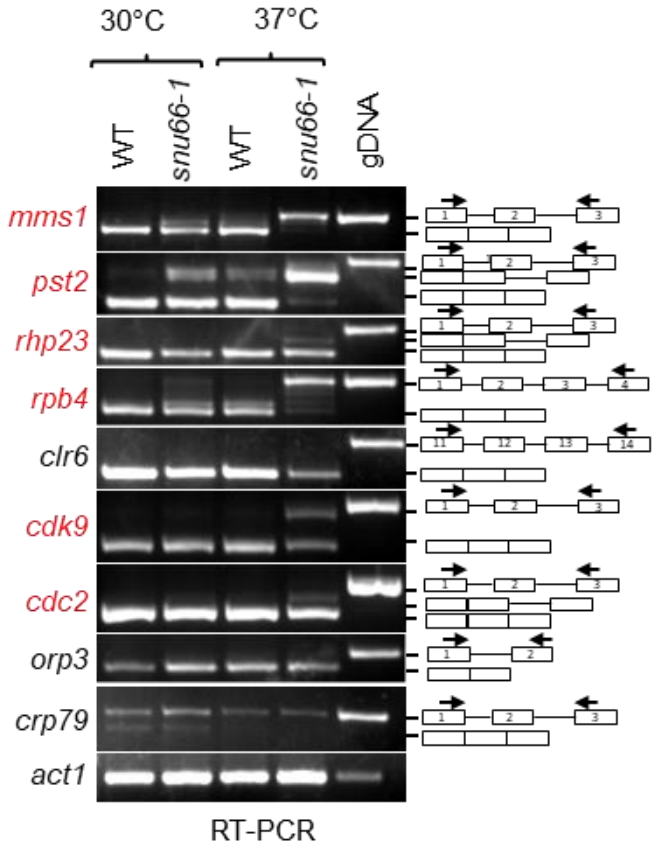

Fig.3.3.2 RT-PCR assays to monitor accumulation of intron-containing transcripts in WT and *snu66-1* mutant at 30°C and 37°C of different *S. pombe* genes using specific set of primers (black arrows) spanning certain introns. The exon number is indicated within the blocks.

Chapter-4

Discussion and Conclusion

The spliceosome although has common evolutionary origins with the group II self-splicing introns, has evolved in such a way that it's assembly, activation and regulation is dependent on a plethora of trans-acting factors. Snu66 is one such splicing factor which being a tri-snRNP component is also associated with the core components of the spliceosome like Prp8 and Brr2. It has been reported that Snu66 acts like a scaffold in the spliceosome helping in the structural organization of the components of the spliceosomal core like Prp8, Prp6, Brr2 that eventually help the spliceosome adopt the active site conformation for catalysis (Zhan et al., 2018). The SIND helps in the usage of a specific non-canonical 5'ss (GUAUAU) and the mutant is not defective in the usage of another non-canonical one (GUCUGU). This suggests a mechanism by which this domain of a splicing factor which in general is defective in the usage of both the non-canonical 5'splice sites can modify the spliceosome's first step catalytic conformation prior to branching reaction.

The human spliceosome structure identified Snu66 in close proximity to RBM42 which is reported to stabilize the U4/U6 stem I capped by the quasi-pseudoknot (Charenton et al., 2019). The same structure suggests Snu66 in association with SNRNP-27K and Prp8 to be involved in solidifying the association of U4 snRNP in tri-snRNP before Brr2 relocation (Charenton et al., 2019). Therefore, with multiple surfaces for interaction to many factors, Snu66 (SIND being one such surface) can play a key role in helping the spliceosomal transitions from pre-B to B to B^{act} to B* complexes.

Snu66 has been reported to genetically interact with Prp8 alleles like *prp8-101* and *prp8** (Mishra et al., 2011). Prp8-101 is a first step allele which makes the spliceosome adopt a conformation such that the branching reaction kinetics quicken while the ligation step slows down (L. Liu et al., 2007). *prp8** (P1348L) shows synthetic lethality with the alternative splicing factor Hub1 (Mishra et al., 2011). The E1960K mutation for *prp8-101* falls in the RNase H domain of Prp8 which is crucial for the catalytic activation of the spliceosome and also, *prp8-101* is defective in the usage of the 5'ss: GUCUGU (Fica & Nagai, 2017; Mishra et al., 2011). So, this mutant is more likely to be influencing the branching catalysis in association with the U6 snRNA. With these genetic links to splicing and the observation of SIND's non-

canonical splicing defects, it is attractive to hypothesise that SIND might also function in association with Prp8 to modify the spliceosome for the formation of the active site for catalysis as well as a factor that can regulate the kinetic proof-reading mechanism in splicing. To this end, we are proceeding to understand the genetic interaction of SIND mutants with Prp8 alleles.

Further, we are planning to address the question of what is the mechanism by which SIND is modifying the spliceosome in *S. pombe* by two approaches. In the first case, we have tagged the splicing factor Cdc5 with HA (for a spliceosomal pull down) in WT and *snu66-1* strains. We will immuno-precipitate Cdc5-6HA and do a Mass-spectrometry analysis to see whether SIND selectively modifies the spliceosome. In the second approach, since it has been reported that the Snu66 C-term extensively interacts with Brr2 (Nguyen et al., 2016), we aim to check whether the Brr2 levels in the spliceosome is affected in SIND mutants. For this, we plan to do a similar spliceosomal pull down with Cdc5-6HA and monitor the levels of Brr2-9myc (WB: anti-myc). The Brr2 levels getting affected in SIND mutant would give us insights into whether SIND helps in the conformational toggling of the tri-snRNP components, particularly Brr2, with the coupling of 5'ss – ACAGAGA pairing and U4/U6 duplex unwinding prior to the branching conformation.

References

Bai, R., Wan, R., Yan, C., Lei, J., & Shi, Y. (2018). Structures of the fully assembled Saccharomyces cerevisiae spliceosome before activation. *Science*, *360*(6396), 1423–1429. https://doi.org/10.1126/science.aau0325

Breathnach, R., & Chambon, P. (1981). Organization and Expression of Eucaryotic Split Genes Coding for Proteins. *Annual Review of Biochemistry*, *50*(1), 349–383. https://doi.org/10.1146/annurev.bi.50.070181.002025

Charenton, C., Wilkinson, M. E., & Nagai, K. (2019). Mechanism of 5' splice site transfer for human spliceosome activation. *Science*, *364*(6438), 362–367. https://doi.org/10.1126/science.aax3289

Fatores, H., & Ao, A. (2011). *Structure of a yeast catalytic step I spliceosome\n\n*. *2235*(6302), 1–5. https://doi.org/10.7910/DVN/PBLJXJ

Fica, S. M., Mefford, M. A., Piccirilli, J. A., & Staley, J. P. (2014). Evidence for a group II intron-like catalytic triplex in the spliceosome. *Nature Structural and Molecular Biology*, *21*(5), 464–471. https://doi.org/10.1038/nsmb.2815

Fica, S. M., & Nagai, K. (2017). Cryo-electron microscopy snapshots of the spliceosome: Structural insights into a dynamic ribonucleoprotein machine. *Nature Structural and Molecular Biology*, *24*(10), 791–799. https://doi.org/10.1038/nsmb.3463

Fica, S. M., Oubridge, C., Galej, W. P., Wilkinson, M. E., Bai, X. C., Newman, A. J., & Nagai, K. (2017). Structure of a spliceosome remodelled for exon ligation. *Nature*, *542*(7641), 377–380. https://doi.org/10.1038/nature21078

Fica, S. M., Tuttle, N., Novak, T., Li, N. S., Lu, J., Koodathingal, P., Dai, Q., Staley, J. P., & Piccirilli, J. A. (2013). RNA catalyses nuclear pre-mRNA splicing. *Nature*, *503*(7475), 229–234. https://doi.org/10.1038/nature12734

Inada, M., & Pleiss, J. A. B. T.-M. in E. (2010). Chapter 3 - Genome-Wide Approaches to Monitor Pre-mRNA Splicing. In *Guide to Yeast Genetics: Functional Genomics, Proteomics, and Other Systems Analysis* (Vol. 470, pp. 51–75). Academic Press. https://doi.org/https://doi.org/10.1016/S0076-6879(10)70003-3

Knop, M., Siegers, K., Pereira, G., Zachariae, W., Winsor, B., Nasmyth, K., & Schiebel, E. (1999). Epitope tagging of yeast genes using a PCR-based strategy: More tags and

improved practical routines. *Yeast*, *15*(10 B), 963–972. https://doi.org/10.1002/(SICI)1097-0061(199907)15:10B<963::AID-YEA399>3.0.CO;2-W

Lesser, C. F., & Guthrie, C. (1993). Mutational analysis of pre-mRNA splicing in Saccharomyces cerevisiae using a sensitive new reporter gene, CUP1. *Genetics*, *133*(4), 851–863.

Li, X., Liu, S., Zhang, L., Issaian, A., Hill, R. C., Espinosa, S., Shi, S., Cui, Y., Kappel, K., Das, R., Hansen, K. C., Zhou, Z. H., & Zhao, R. (2019). A unified mechanism for intron and exon definition and back-splicing. *Nature*, *573*(7774), 375–380. https://doi.org/10.1038/s41586-019-1523-6

Li, Z., Lee, I., Moradi, E., Hung, N. J., Johnson, A. W., & Marcotte, E. M. (2009). Rational extension of the ribosome biogenesis pathway using network-guided genetics. *PLoS Biology*, *7*(10). https://doi.org/10.1371/journal.pbio.1000213

Liu, L., Query, C. C., & Konarska, M. M. (2007). Opposing classes of prp8 alleles modulate the transition between the catalytic steps of pre-mRNA splicing. *Nature Structural and Molecular Biology*, *14*(6), 519–526. https://doi.org/10.1038/nsmb1240

Liu, S., Li, X., Zhang, L., Jiang, J., Hill, R. C., Cui, Y., Hansen, K. C., Zhou, Z. H., & Zhao, R. (2017). Structure of the yeast spliceosomal postcatalytic P complex. *Science*, *358*(6368), 1278–1283. https://doi.org/10.1126/science.aar3462

Mishra, S. K., Ammon, T., Popowicz, G. M., Krajewski, M., Nagel, R. J., Ares, M., Holak, T. A., & Jentsch, S. (2011). Role of the ubiquitin-like protein Hub1 in splice-site usage and alternative splicing. *Nature*, *474*(7350), 173–180. https://doi.org/10.1038/nature10143

Neufeld, N., Brody, Y., & Shav-tal, Y. (2014). *Spliceosomal Pre-mRNA Splicing*. *1126*(310), 257–269. https://doi.org/10.1007/978-1-62703-980-2

Nguyen, T. H. D., Galej, W. P., Bai, X. C., Oubridge, C., Newman, A. J., Scheres, S. H. W., & Nagai, K. (2016). Cryo-EM structure of the yeast U4/U6.U5 tri-snRNP at 3.7 Å resolution. *Nature*, *530*(7590), 298–302. https://doi.org/10.1038/nature16940

Plaschka, C., Lin, P. C., Charenton, C., & Nagai, K. (2018). Prespliceosome structure provides insights into spliceosome assembly and regulation. *Nature*, *559*(7714), 419–422. https://doi.org/10.1038/s41586-018-0323-8

Plaschka, C., Lin, P. C., & Nagai, K. (2017). Structure of a pre-catalytic spliceosome. *Nature*, *546*(7660), 617–621. https://doi.org/10.1038/nature22799

Shi, Y. (2017a). Mechanistic insights into precursor messenger RNA splicing by the spliceosome. *Nature Reviews Molecular Cell Biology*, *18*(11), 655–670. https://doi.org/10.1038/nrm.2017.86

Shi, Y. (2017b). The Spliceosome: A Protein-Directed Metalloribozyme. *Journal of Molecular Biology*, *429*(17), 2640–2653. https://doi.org/10.1016/j.jmb.2017.07.010

Staley, J. P., & Guthrie, C. (1999). An RNA switch at the 5' splice site requires ATP and the DEAD box protein Prp28p. *Molecular Cell*, *3*(1), 55–64. https://doi.org/10.1016/S1097-2765(00)80174-4

Steitz, T. A., & Steitz, J. A. (1993). A general two-metal-ion mechanism for catalytic RNA. *Proceedings of the National Academy of Sciences of the United States of America*, *90*(14), 6498–6502. https://doi.org/10.1073/pnas.90.14.6498

Stevens, S W, Barta, I., Ge, H. Y., Moore, R. E., Young, M. K., Lee, T. D., & Abelson, J. (2001). Biochemical and genetic analyses of the U5, U6, and U4/U6.U5 sStevens, S. W., Barta, I., Ge, H. Y., Moore, R. E., Young, M. K., Lee, T. D., & Abelson, J. (2001). Biochemical and genetic analyses of the U5, U6, and U4/U6.U5 small nuclear ribonucleoproteins. *Rna*, *7*(11), 1543–1553.

Stevens, Scott W., & Abelson, J. (1999). Purification of the yeast U4/U6·U5 small nuclear ribonucleoprotein particle and identification of its proteins. *Proceedings of the National Academy of Sciences of the United States of America*, *96*(13), 7226–7231. https://doi.org/10.1073/pnas.96.13.7226

Wahl, M. C., Will, C. L., & Lührmann, R. (2009). The Spliceosome: Design Principles of a Dynamic RNP Machine. *Cell*, *136*(4), 701–718. https://doi.org/10.1016/j.cell.2009.02.009

Wan, R., Bai, R., Yan, C., Lei, J., & Shi, Y. (2019). Structures of the Catalytically Activated Yeast Spliceosome Reveal the Mechanism of Branching. *Cell*, *177*(2), 339-351.e13. https://doi.org/10.1016/j.cell.2019.02.006

Wan, R., Yan, C., Bai, R., Lei, J., & Shi, Y. (2017). Structure of an Intron Lariat Spliceosome from Saccharomyces cerevisiae. *Cell*, *171*(1), 120-132.e12.

https://doi.org/10.1016/j.cell.2017.08.029

Wilkinson, M. E., Charenton, C., & Nagai, K. (2020). RNA Splicing by the Spliceosome. *Annual Review of Biochemistry*, *89*(1), 1–30. https://doi.org/10.1146/annurev-biochem-091719-064225

Yan, C., Wan, R., Bai, R., Huang, G., & Shi, Y. (2016). Structure of a yeast activated spliceosome at 3.5 Å resolution. *Science*, *353*(6302), 904–912. https://doi.org/10.1126/science.aag0291

Yan, C., Wan, R., Bai, R., Huang, G., & Shi, Y. (2017). Structure of a yeast step II catalytically activated spliceosome. *Science*, *355*(6321), 149–155. https://doi.org/10.1126/science.aak9979

Zhan, X., Yan, C., Zhang, X., Lei, J., & Shi, Y. (2018). Structures of the human pre-catalytic spliceosome and its precursor spliceosome. *Cell Research*, *28*(12), 1129–1140. https://doi.org/10.1038/s41422-018-0094-7

Appendix

Strain list

Stock ID	Relevant genotype
S. cerevisiae strains	
pJ69-7a	trp1-901 leu2-3,112 ura3-53 his3-200 gal4 gal80 GAL1::HIS3 GAL2- ADE2 met2::GAL7-lacZ
W303	ho ade2-1 his3-11, 15 leu2-3, 112 ura3 trp1-1 ssd1 can1-100
yJU75	MATa ade2 cup1Δ::ura3 his3 leu2 lys2 prp8Δ::LYS2 trp1:pJU169
PCB001	yJU75 *snu66::NatNT2*
PCB002	yJU75 *snu66::NatNT2 snu66::KANMX6*
PCB003	yJU75 *snu66 RRAA::KANMX6*
PCB004	yJU75 *snu66 D533A::KANMX6*
PCB005	yJU75 *snu66 K546A::KANMX6*
PCB006	yJU75 *snu66 ΔSIND::KANMX6*
S. pombe strains	
SP1	h- ade6-M216, leu1, ura4-D18
SP7	JY741 snu66-1::ura4+
SP7*	JY741 snu66-1::ura4-

Plasmid list

Stock ID	Plasmid
D001	pGADC1 EV
D002	pGBDUC1 EV
pRB001	pGADC1 Sap1_FL
pRB002	pGBDUC1 Snu66_FL
pRB003	pGADC1 Sap1 I236A
pBR004	pGADC1 Sap1 K546A
pBR005	pGADC1 Sap1 521-end (shorter form)
pBR006	pGBDUC1 Snu66 ΔHIND
pBR007	pGBDUC1 Snu66 180-587
pBR008	pGBDUC1 Snu66 267-587

pBR009	pGBDUC1 Snu66 412-587
pBR010	pGBDUC1 Snu66-SIND
pSKM355	pGAD Sap1-3myc delta SIM
pSKM321	pGAD C1 Sap1 583-end
pSKM323	pGAD C1 Sap1 568-*
pSKM447	pGBDU C1 Snu66 525-554
pSKM448	pGAD C1 Snu66 518-554
pSKM462	pGBDU C1 Snu66 531-554
pSKM404	YE112 pADH-3myc-Snu66 tADH
pSKM420	YE112 pADH-3myc-Snu66 delta75-87
pSKM421	YE112 pADH-3myc-Snu66 delta102-113
pSKM422	YE112 pADH-3myc-Snu66 delta126-128
pSKM423	YE112 pADH-3myc-Snu66 delta161-183
pSKM424	YE112 pADH-3myc-Snu66 delta437-460
pSKM425	YE112 pADH-3myc-snu66 delta365-394 tADH
pSKM426	YE112 pADH-3myc-snu66 delta321-351 tADH
pSKM427	YE112 pADH-3myc-snu66 delta297-320 tADH
pSKM428	YE112 pADH-3myc-snu66 delta273-295 tADH
pSKM429	YE112 pADH-3myc-Snu66 delta sbm tADH #2

pSKM430	YE112 pADH-3myc-Snu66 delta hbm delta sbm tADH
pSKM440	YE112 pADH-3myc-Snu66 RRAA tADH
pBR011	YC22-pU6-U6 snRNA FL
pBR012	YC22- U6 snRNA G50A
pBR013	YC22-U6 G50C
pBR014	YC22-U6 G50T
pBR015	YC22-U6 C48A
pBR016	YC22-U6 C48G
pBR017	YC22-U6 C48T
pBR018	peno-3MYC–ura4 (tho5-i1)
pBR019	peno-3MYC–ura4 (tho5-i1 5'ss: GUAUAU)
pBR020	peno-3MYC–ura4 (tho5-i1 bp: TTAAC)
pBR021	peno-3MYC–ura4 (tho5-i1 bp: CTAAA)
pBR022	peno-3MYC–ura4 (tho5-i1 3'ss: AAG)

RT-PCR primers

Gene name	**Primer ID**	**Sequence**
mms1	SKM PR_2282	GCAACTCCCAAGAGATTACTTG
	SKM PR_2283	GCGAAGTTCTATAGCATTGCTG
pst2	SKM PR_2594	ATGGAACAAACACTAGCGATATTAA
	SKM PR_2595	GAAGTTGGCACCGCTATTCG
rhp23	SKM PR_2596	GAATTTGACATTCAAAAATCTACAGCAG
	SKM PR_2597	GTGCTTCACTAGTGGCAGTAG
clr6	SKM PR_2600	GGGCTGTACGAATTTTGTTC
	SKM PR_2601	CCTGTTCCAATTCCGGTGTC
cdk9	SKM PR_2606	GAAACGCTCAAGCAGCGTTTC
	SKM PR_2607	GAACCACGACGTCGATGCTTC
rpb4	SKM PR_2604	GCCGAGGGCTATTTTTGAGG
	SKM PR_2605	CGCAAAGTGGAAAGCTCATC
crp79	SKM PR_2608	GTCCCCGGACAGTATGAAGATG

	SKM PR_2609	CAGTGATTGACGTATCGTTAGG
orp3	SKM PR_2610	GTCAGCAATACTACAATATGATTCAG
	SKM PR_2611	CAAAACTCTGGCGTTACTATC
cdc2	SKM PR_2612	CTGAGGGAGTTCCTAGCACAGC
	SKM PR_2613	GATCCCAACAATACTTCAGGAG
act1	SKM PR_13	CCCCTAGAGCTGTATTCCC
	SKM PR_14	CCAGTGGTACGACCAGAGG